
Recommended Citation

Shu-Jin Li, Zhi-Kang Cao, Wen-Kai Wang, Xiao-Han Zhang, Xing-De Xiang. Functional Sulfate Electrolytes Enable the Enhanced Cycling Stability of $\text{NaTi}_2(\text{PO}_4)_3/\text{C}$ Anode Material for Aqueous Sodium-Ion Batteries[J]. *Journal of Electrochemistry*, 2021, 27(6): 605-613.

DOI: Aqueous sodium-ion batteries show promising application in fields of large-scale storage of intermittent renewable energies owing to the earth-abundant sodium resources and incombustible aqueous electrolytes. Primary factors determining whether they can be commercially utilized are low cost and long lifetime. Among current electrode materials, NASICON-type $\text{NaTi}_2(\text{PO}_4)_3$ arouses wide interests

material for aqueous sodium-ion batteries as it offers a high specific capacity, fast Na-transport ability and reasonable working potential, however, suffering from insufficient cycling

performance caused by severe dissolution of active materials in traditional aqueous electrolytes. In this work, a functional sulfate electrolyte ($2 \text{ mol}\cdot\text{L}^{-1} \text{ Na}_2\text{SO}_4 + 0.3 \text{ mol}\cdot\text{L}^{-1} \text{ MgSO}_4$) was designed by coupling concentrated Na_2SO_4 salt and functional MgSO_4 additive to enhance the cycling stability of

$\text{NaTi}_2(\text{PO}_4)_3/\text{C}$ material. Experimental results from cyclic voltammetry and galvanostatic measurements suggest that the electrolyte can improve electrochemical reversibility and cycling performance of

$\text{NaTi}_2(\text{PO}_4)_3/\text{C}$ material relative to traditional electrolyte ($1 \text{ mol}\cdot\text{L}^{-1} \text{ Na}_2\text{SO}_4$). In specific, the material

harvested a reversible capacity of $93.4 \text{ mAh}\cdot\text{g}^{-1}$ and impressive capacity retention of 96.5% at the specific current of $100 \text{ mA}\cdot\text{g}^{-1}$ in the functional sulfate electrolyte, but exhibited a reversible capacity of 88.6

Wen-Kai Wang lower capacity retention of 72.1% in the traditional electrolyte. In order to explore intrinsic causes of the performance improvement, structural properties of the material before and after

$Xiao-Han Zhang$ were comparatively investigated by using X-ray diffraction and X-ray photon spectroscopy. It is found that the material showed excellent structural stability and formation of protective Mg-containing

$Xing-De Xiang$ during cycling in the functional sulfate electrolyte. Both the raised electrolyte-salt

concentration and functional MgSO_4 additive should be responsible for the enhanced structural stability.

College of Chemistry & Chemical Engineering and Resource Utilization, Northeast Forestry University, Harbin 150040, Heilongjiang, China; xiangxinde@nefu.edu.cn

The high electrolyte-salt concentration could decrease electrochemical activity and widen electrochemical stability window of electrolyte solvents, while the MgSO_4 additive could timely capture the hydroxyl group resulting from water-solvent decomposition to prevent the alkalization of aqueous electrolytes and spontaneously form protective Mg(OH)_2 interfaces. As a result, the electrolyte could suppress the dissolution of active $\text{NaTi}_2(\text{PO}_4)_3$, thus, resulting in the enhanced structural stability and cycling performance. With an aim to further exhibit the feasibility for practical application, full aqueous sodium-ion batteries were assembled by coupling $\text{Na}_2\text{Ni}[\text{Fe}(\text{CN})_6]$ cathode, functional sulfate electrolyte and $\text{NaTi}_2(\text{PO}_4)_3/\text{C}$ anode. Charge/discharge tests show that the battery could deliver a working voltage of 1.3 V and a reversible capacity of $84.2 \text{ mAh}\cdot\text{g}^{-1}$ (calculated as the mass of active anode material) at the current of $100 \text{ mA}\cdot\text{g}^{-1}$, achieving a specific energy of about $110 \text{ Wh}\cdot\text{kg}^{-1}$. After being continuously

charging and discharging for 500 cycles at the current of $500 \text{ mA}\cdot\text{g}^{-1}$, it achieved high capacity retention of 80%. The results in this work suggest that designing functional additive-containing sulfate electrolytes is an effective strategy to fabricate low-cost, long-lifetime aqueous sodium-ion batteries.

Available at: <https://jelectrochem.xmu.edu.cn/journal/vol27/iss6/4>

硫酸盐功能电解液增强水系钠离子电池 $\text{NaTi}_2(\text{PO}_4)_3/\text{C}$ 负极材料电化学性能的研究

李姝谨, 曹志康, 王文凯, 张晓菡, 向兴德*

(东北林业大学, 化学化工与资源利用学院, 黑龙江 哈尔滨 150040)

摘要: 水系钠离子电池具有钠资源丰富、成本低廉、安全可靠、维护简单等特点, 在可再生能源规模储存领域具有重要应用前景。NASICON型 $\text{NaTi}_2(\text{PO}_4)_3$ 具有可逆容量高、工作电位低、离子传输快等优点, 是目前最受关注的水系钠离子电池负极材料。但是, 该材料在传统的水系电解液中结构不稳定, 循环性能不足。本论文通过调控 Na_2SO_4 浓度和引入 MgSO_4 添加剂, 构建了一种新型硫酸盐功能电解液($2 \text{ mol}\cdot\text{L}^{-1} \text{ Na}_2\text{SO}_4 + 0.3 \text{ mol}\cdot\text{L}^{-1} \text{ MgSO}_4$)。该电解液能够显著增强 $\text{NaTi}_2(\text{PO}_4)_3/\text{C}$ 材料在充放电循环过程中的结构稳定性, 从而提高其电化学可逆性和稳定性。电化学测试表明, $\text{NaTi}_2(\text{PO}_4)_3/\text{C}$ 基于该电解液在 $100 \text{ mA}\cdot\text{g}^{-1}$ 条件下的可逆容量为 $93.4 \text{ mAh}\cdot\text{g}^{-1}$, 循环 100 次后容量保持率高达 96.5%; 基于该电解液构建的 $\text{Na}_2\text{Ni}[\text{Fe}(\text{CN})_6]\text{NaTi}_2(\text{PO}_4)_3/\text{C}$ 电池可以稳定循环 500 次以上。本论文结合 XRD、XPS 等技术讨论分析了该电解液的功能作用机制, 其研究结果为设计低成本高性能水系钠离子电池提供了新思路和实验基础。

关键词: 水系钠离子电池; 负极材料; 硫酸盐电解液; 结构稳定性; 循环性能

1 引言

发展和利用可再生能源(如太阳能、风能等)是解决能源短缺和环境污染的有效途径。但是, 可再生能源易受气候、天气、地理等自然因素影响, 发电不稳定, 不能直接并网使用。水系可充电池是一种低成本高安全的电化学储能技术, 在可再生能源规模储存领域具有应用前景。目前, 水系可充电池主要包括已商业化使用的酸性电池(如铅酸电池)、碱性电池(如镍氢电池)及新兴的中性电池(如碱金属离子电池)。其中, 水系钠离子电池凭借钠资源丰富、能量转换效率高、环境友好、自放电小等优势, 近年来受到了人们的广泛关注^[1-3]。它主要由正极材料、负极材料和水系电解液组成, 其电化学反应原理与锂离子电池相似。充电时, 正极材

料发生氧化反应, 失去电子, 同时脱出钠离子; 电子通过外电路传输到负极, 同时钠离子经过电解液迁移到负极; 负极材料得到电子, 同时嵌入钠离子, 发生还原反应^[4]。放电过程与充电过程相反。循环寿命长及综合成本低是水系钠离子电池在规模储能领域商业化使用的先决条件。这要求水系钠离子电池使用电化学活性高、结构稳定性强及原料成本低的电池材料。目前, 可用于水系钠离子电池的正极材料主要有过渡金属氧化物^[5-7]、聚阴离子化合物^[8-11]和普鲁士蓝类化合物^[12-15], 负极材料主要有钛基磷酸盐^[16-18]和聚酰亚胺^[19, 20], 常用电解液有 Na_2SO_4 、 NaClO_4 和 NaSO_3CF_3 。

NASICON型 $\text{NaTi}_2(\text{PO}_4)_3$ 具有电化学活性高、离子传输快、反应电位适中等特点, 是一类有前景

引用格式: Li S J, Cao Z K, Wang W K, Zhang X H, Xiang X D. Functional sulfate electrolytes enable the enhanced cycling stability of $\text{NaTi}_2(\text{PO}_4)_3/\text{C}$ anode material for aqueous sodium-ion batteries. *J. Electrochem.*, 2021, 27(6): 605-613.

的水系钠离子电池负极材料^[21-23]。但是,它在传统水系电解液中结构不稳定,易发生溶解,循环性能不足。Whitacre 课题组^[24]研究了水溶液 pH 值对 $\text{NaTi}_2(\text{PO}_4)_3$ 结构稳定性的影响,发现 $\text{pH} = 9 \sim 14$ 的溶液均能造成材料发生不同程度的化学溶解,并在材料表面生成电化学惰性的钛基氧化物杂相。 pH 增加(即碱性化)会加剧材料的结构衰退。Shirpour 课题组^[25]研究了 $\text{NaTi}_2(\text{PO}_4)_3$ 基于传统 Na_2SO_4 电解液在充放电循环过程中的物质结构及反应动力学变化,揭示了其容量衰减机理: $\text{NaTi}_2(\text{PO}_4)_3$ 在水系电解液中易溶出部分 Na^+ 离子和 Ti^{4+} 离子;溶出的 Ti^{4+} 与硫酸根离子反应生成无定形 $\text{Ti}(\text{SO}_4)_2$ 沉淀及其水解产物 H_2TiO_3 。这些副反应产物容易堵塞离子传输通道,降低材料在循环过程中的反应动力学。目前,提高 $\text{NaTi}_2(\text{PO}_4)_3$ 电化学性能的主要策略有表面碳包覆^[26-28]、阳离子掺杂^[29-31]和设计高浓度电解液^[32-34]。表面碳包覆不仅可以提高材料电子传导性,而且可以减少活性材料与电解液的直接接触,从而提高材料的电化学性能。但是, $\text{NaTi}_2(\text{PO}_4)_3$ 的嵌钠电位接近电解液电化学窗口的下限,容易诱导电解液在充放电过程中发生还原析氢反应,导致电解液碱性化,从而加剧材料的化学溶解。因此, $\text{NaTi}_2(\text{PO}_4)_3/\text{C}$ 经过一定循环后会出现明显的容量衰退。掺杂非活性阳离子(如 Mg^{2+} 、 Mn^{2+} 、 V^{3+} 等)有利于增强材料的结构稳定性和耐腐蚀性,从而提高材料在水系电解液中的循环性能,但是会大大降低材料的可逆容量。另外,设计高浓度电解液有利于拓宽电解液的电化学稳定窗口,提升电极/电解液界面稳定性,增强材料的电化学可逆性和循环性能。但是,可用于配制高浓度电解液的钠盐仅有易制爆的 NaClO_4 和价格昂贵的 NaSO_3CF_3 ,而低成本的 Na_2SO_4 溶解度有限,难以配制高浓度电解液。

本论文基于调控 Na_2SO_4 浓度和引入 MgSO_4 添加剂构建了一种有利于增强 $\text{NaTi}_2(\text{PO}_4)_3$ 循环稳定性的新型硫酸盐功能电解液。实验结果表明, $\text{NaTi}_2(\text{PO}_4)_3$ 基于这种电解液在 $100 \text{ mA} \cdot \text{g}^{-1}$ 条件下循环 100 次后容量保持率可以高达 96.5%。此外,结合 X 射线衍射和 X 射线光电子能谱等技术探讨了该电解液的功能作用机制。

2 实 验

2.1 试剂与仪器

柠檬酸($\text{C}_6\text{H}_8\text{O}_7 \cdot \text{H}_2\text{O}$,纯度 99.5%,天津市光复

精细化工研究所),乙酸钠(CH_3COONa ,纯度 99.0%)、磷酸二氢铵($\text{NH}_4\text{H}_2\text{PO}_4 \cdot 2\text{H}_2\text{O}$,纯度 $\geq 99.0\%$)、氯化镍($\text{NiCl}_2 \cdot 6\text{H}_2\text{O}$,纯度 99.9%)、亚铁氰化钠($\text{Na}_4\text{Fe}(\text{CN})_6 \cdot 10\text{H}_2\text{O}$,纯度 99.9%)均购自上海阿拉丁生化科技股份有限公司。

X 射线衍射仪(X'Pert Powder, 荷兰帕纳科公司),X 射线光电子能谱(KRATOS, 日本岛津制作所),电化学工作站(CHI600E, 上海辰华仪器有限公司),电池测试系统(CT2001A, 武汉蓝电电子股份有限公司)。

2.2 材料制备与分析

采用溶胶凝胶法制备 $\text{NaTi}_2(\text{PO}_4)_3/\text{C}$ 负极材料:称取 0.3164 g 柠檬酸、0.2659 g 乙酸钠、1.1185 g 磷酸二氢铵,加入 30 mL 去离子水中,磁力搅拌 5 min,使其完全溶解;缓慢加入钛酸异丙酯溶液(3 mL 无水乙醇 + 2 mL 钛酸异丙酯),搅拌 20 min 后,加热至 80 °C 进行蒸发,直至形成凝胶。将凝胶放入真空干燥箱中,100 °C 干燥 12 h,然后研磨均匀,获得样品前驱体;将前驱体粉末送入管式炉(Ar 气氛围),450 °C 预烧 4 h,750 °C 反应 8 h,升温速率为 $10 \text{ }^{\circ}\text{C} \cdot \text{min}^{-1}$,即可得到 $\text{NaTi}_2(\text{PO}_4)_3/\text{C}$ 负极材料。

采用化学沉淀法制备 $\text{Na}_2\text{Ni}[\text{Fe}(\text{CN})_6]$ 正极材料:首先,称取 2.3793 g 氯化镍,溶解于 100 mL 去离子水中,记为溶液 A;然后称取 4.8406 g 亚铁氰化钠,溶解于 100 mL 蒸馏水中,记为溶液 B。在搅拌条件下将溶液 A 缓慢滴入溶液 B 中。将所得的悬浮液在 $500 \text{ r} \cdot \text{min}^{-1}$ 转速下搅拌 6 h,然后静置 24 h。然后反复离心分离洗涤(蒸馏水洗 3 次,乙醇洗 2 次),最后在真空烘箱中 60 °C 干燥 24 h,即可得到 $\text{Na}_2\text{Ni}[\text{Fe}(\text{CN})_6]$ 正极材料。

材料结构表征:通过 X 射线衍射仪(XRD)分析材料循环前后的结构性质。运用 X 射线光电子能谱(XPS,电压 15 kV,电流 5 mA)分析材料循环前后的表面物质结构及元素价态。循环后的电极材料在表征前需用去离子水多次冲洗,然后自然风干。基于 $\text{NaTi}_2(\text{PO}_4)_3$ 的热稳定性及碳的可燃性,采用简单的燃烧法测定 $\text{NaTi}_2(\text{PO}_4)_3/\text{C}$ 材料中的碳含量(将 0.1 g 样品在 800 °C 条件下(空气氛围)处理 4 h,计算处理前后的质量损失)。

工作电极制备:将活性物质($\text{NaTi}_2(\text{PO}_4)_3/\text{C}$)、导电剂(Super P)和粘结剂(PVDF)按质量比 7:2:1 进行混合,加入少量氮甲基吡咯烷酮(NMP,电池级,

天津光复),通过研磨制成均匀的浆料,然后涂覆在钛片上,在真空烘箱中80℃干燥8 h。单个极片的活性物质载量约 $2 \text{ mg} \cdot \text{cm}^{-2}$ 。

材料电化学性质测试:以工作电极、 Ag/AgCl (饱和KCl溶液)参比电极、 $\text{Na}_2\text{Ni}[\text{Fe}(\text{CN})_6]$ 辅助电极和 Na_2SO_4 溶液构建三电极测试体系。利用电化学工作站测试循环伏安曲线,电位窗口-1.0~0 V,扫描速率 $0.1 \text{ mV} \cdot \text{s}^{-1}$ 。运用充放电测试系统测试材料的电化学性能,电位窗口为-1.0~0 V,电流密度为 $100 \text{ mA} \cdot \text{g}^{-1}$ 。

钠离子电池性能测试:以 $\text{NaTi}_2(\text{PO}_4)_3/\text{C}$ 负极、 $\text{Na}_2\text{Ni}[\text{Fe}(\text{CN})_6]$ 正极和 Na_2SO_4 电解液组装2032型扣式电池,其中,正极材料与负极材料的质量比为1.8:1。利用充放电测试系统进行恒流充放电测试,电压窗口为0.6~1.6 V,电流密度为 $100 \text{ mA} \cdot \text{g}^{-1}$ 。

3 结果与讨论

NASICON型 $\text{NaTi}_2(\text{PO}_4)_3$ 属于六方晶系,空间群R-3c,由 TiO_6 八面体和 PO_4 四面体结构单元共角交联而成,具有三维的钠离子传输通道^[35]。从图1可以看出,材料样品在 14.5° 、 20.3° 、 20.9° 、 24.2° 、 29.2° 、 32.3° 和 36.7° 处出现了较强的XRD衍射峰,与标准卡片完全吻合,分别对应于(012)、(104)、(110)、(113)、(024)、(116)和(300)晶面。材料的晶胞常数为 $a=b=8.47 \text{ \AA}$, $c=22.00 \text{ \AA}$,与文献值一致^[35]。通过燃烧法测定材料中的碳含量为4.3wt.%。这说明成功合成出了高纯相的 $\text{NaTi}_2(\text{PO}_4)_3/\text{C}$ 材料。

利用循环伏安法研究了 $\text{NaTi}_2(\text{PO}_4)_3/\text{C}$ 材料基

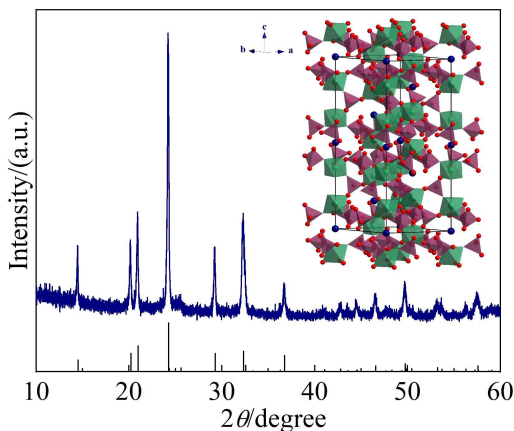


图1 $\text{NaTi}_2(\text{PO}_4)_3/\text{C}$ 材料的X射线衍射图和结构示意图(网络版彩图)

Figure 1 XRD pattern and schematic structure of $\text{NaTi}_2(\text{PO}_4)_3/\text{C}$ material (color on line)

于硫酸盐功能电解液的电化学性质。图2对比展示了它在 $1 \text{ mol} \cdot \text{L}^{-1} \text{ Na}_2\text{SO}_4$ 、 $2 \text{ mol} \cdot \text{L}^{-1} \text{ Na}_2\text{SO}_4$ 、 $2 \text{ mol} \cdot \text{L}^{-1} \text{ Na}_2\text{SO}_4 + 0.3 \text{ mol} \cdot \text{L}^{-1} \text{ MgSO}_4$ 不同电解液中的循环伏安曲线。在-0.8 V附近出现一对氧化还原峰。还原峰对应于伴有钠离子嵌入的 Ti^{4+} 还原反应,氧化峰归因于伴有钠离子脱出的 Ti^{3+} 氧化反应^[26]。在 $1 \text{ mol} \cdot \text{L}^{-1} \text{ Na}_2\text{SO}_4$ 电解液中(图2(A)),循环1圈后,峰电流明显减小,且出现氧化峰正移、还原峰负移的极化增强现象。峰电流减小主要是由于活性材料的溶解,而极化增强是因为溶解副产物覆盖在材料表面,阻碍钠离子传输,降低了材料的反应动力学^[25]。当 Na_2SO_4 浓度增加至 $2 \text{ mol} \cdot \text{L}^{-1}$ (准饱和状态)时(图2(B)),材料在循环过程中的峰电流减小行为有所抑制,峰电位偏移现象不明显。当引入 $0.3 \text{ mol} \cdot \text{L}^{-1} \text{ MgSO}_4$ 添加剂后(图2(C)),材料在 Na_2SO_4 电解液中循环3圈后几乎没有出现峰电流减小和峰电位偏移现象。这表明增加电解液浓度和引入 MgSO_4 添加剂能够有效增强 $\text{NaTi}_2(\text{PO}_4)_3/\text{C}$ 在 Na_2SO_4 电解液的电化学稳定性。为了更好展现电解液浓度和添加剂对 $\text{NaTi}_2(\text{PO}_4)_3/\text{C}$ 电化学性质的影响,图2(D)对比展示了 $\text{NaTi}_2(\text{PO}_4)_3/\text{C}$ 在 $1 \text{ mol} \cdot \text{L}^{-1} \text{ Na}_2\text{SO}_4$ 、 $2 \text{ mol} \cdot \text{L}^{-1} \text{ Na}_2\text{SO}_4$ 和 $2 \text{ mol} \cdot \text{L}^{-1} \text{ Na}_2\text{SO}_4 + 0.3 \text{ mol} \cdot \text{L}^{-1} \text{ MgSO}_4$ 电解液中的第3圈循环伏安曲线。从图中可以看出,基于传统的 $1 \text{ mol} \cdot \text{L}^{-1} \text{ Na}_2\text{SO}_4$ 电解液,材料的氧化峰与还原峰电位分别位于-0.712 V和-0.876 V,电位间距约164 mV;当 Na_2SO_4 浓度增加到 $2 \text{ mol} \cdot \text{L}^{-1}$ 时,氧化峰发生负移,且还原峰发生正移,氧化峰与还原峰的电位间距缩小至85 mV。当引入 MgSO_4 添加剂后,氧化峰与还原峰的电位间距继续减小至60 mV。这表明增加电解液浓度和引入 MgSO_4 添加剂有利于提高 $\text{NaTi}_2(\text{PO}_4)_3/\text{C}$ 材料在 Na_2SO_4 电解液中的电化学可逆性。对比结果表明,硫酸盐功能电解液可以增强 $\text{NaTi}_2(\text{PO}_4)_3/\text{C}$ 材料的电化学可逆性和稳定性。

通过恒流充放电测试考察了 $\text{NaTi}_2(\text{PO}_4)_3/\text{C}$ 基于硫酸盐功能电解液的充放电性能。图3对比展示了它在 $1 \text{ mol} \cdot \text{L}^{-1} \text{ Na}_2\text{SO}_4$ 、 $2 \text{ mol} \cdot \text{L}^{-1} \text{ Na}_2\text{SO}_4$ 、 $2 \text{ mol} \cdot \text{L}^{-1} \text{ Na}_2\text{SO}_4 + 0.3 \text{ mol} \cdot \text{L}^{-1} \text{ MgSO}_4$ 不同电解液中的充放电曲线及循环稳定性(在 $100 \text{ mA} \cdot \text{g}^{-1}$ 条件下连续充放100圈)。可以看出,当电解液为传统的 $1 \text{ mol} \cdot \text{L}^{-1} \text{ Na}_2\text{SO}_4$ 时,材料的首圈放电容量为 $113 \text{ mAh} \cdot \text{g}^{-1}$,可逆充放容量为 $88.6 \text{ mAh} \cdot \text{g}^{-1}$,对应的首圈库伦效率为78.4%。容量损失主要源于电解液的

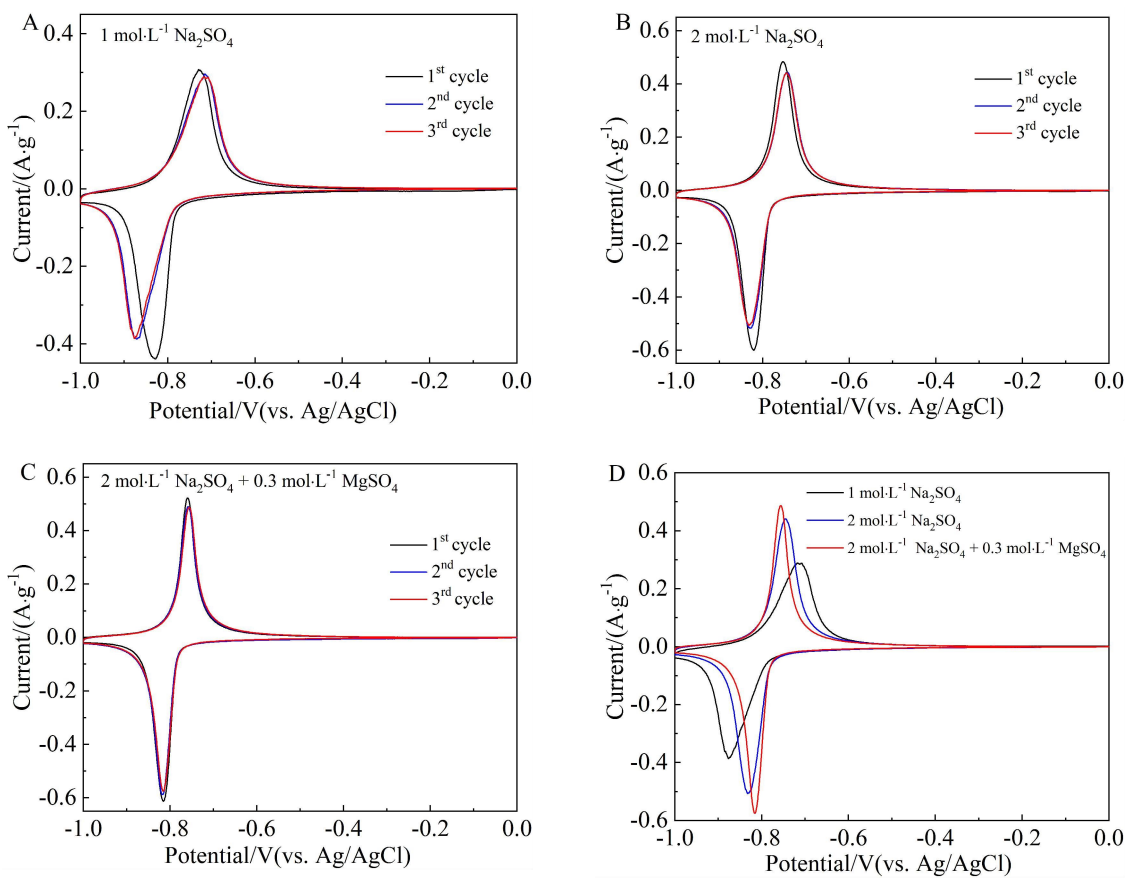


图 2 $\text{NaTi}_2(\text{PO}_4)_3/\text{C}$ 材料基于 Na_2SO_4 电解液的循环伏安曲线:(A) $1 \text{ mol}\cdot\text{L}^{-1} \text{Na}_2\text{SO}_4$ 电解液,(B) $2 \text{ mol}\cdot\text{L}^{-1} \text{Na}_2\text{SO}_4$ 电解液,(C) $2 \text{ mol}\cdot\text{L}^{-1} \text{Na}_2\text{SO}_4 + 0.3 \text{ mol}\cdot\text{L}^{-1} \text{MgSO}_4$ 电解液,(D)不同电解液的对比 (网络版彩图)

Figure 2 Cyclic voltammograms of $\text{NaTi}_2(\text{PO}_4)_3/\text{C}$ material in Na_2SO_4 based electrolytes: (A) $1 \text{ mol}\cdot\text{L}^{-1} \text{Na}_2\text{SO}_4$, (B) $2 \text{ mol}\cdot\text{L}^{-1} \text{Na}_2\text{SO}_4$, (C) $2 \text{ mol}\cdot\text{L}^{-1} \text{Na}_2\text{SO}_4 + 0.3 \text{ mol}\cdot\text{L}^{-1} \text{MgSO}_4$, and (D) comparison in various electrolytes. (color on line)

不可逆分解反应。副反应容易造成电解液碱性化,从而加剧 $\text{NaTi}_2(\text{PO}_4)_3/\text{C}$ 材料的溶解,导致材料可逆容量衰退^[24]。循环 100 次后,材料可逆容量降低至 $63.9 \text{ mAh}\cdot\text{g}^{-1}$,对应的容量保持率仅为 72.1%。当 Na_2SO_4 浓度增加至 $2 \text{ mol}\cdot\text{L}^{-1}$ 时,材料的可逆容量为 $88.9 \text{ mAh}\cdot\text{g}^{-1}$,循环 100 次后容量保持率提高至 83.4%。这是因为增加电解液浓度可以降低水分子的相对含量,改变荷电离子的溶剂化结构,有利于形成稳定的电极/电解液界面,从而抑制电极活性材料溶解^[32]。当引入 $0.3 \text{ mol}\cdot\text{L}^{-1} \text{MgSO}_4$ 添加剂后,可逆容量提升至 $93.4 \text{ mAh}\cdot\text{g}^{-1}$,循环 100 圈后容量保持率高达 96.5%,这说明引入 MgSO_4 添加剂可以有效提高材料在循环过程中的结构稳定性。上述结果表明,硫酸盐功能电解液可以显著增强 $\text{NaTi}_2(\text{PO}_4)_3/\text{C}$ 的循环性能。

为了探究硫酸盐功能电解液增强 $\text{NaTi}_2(\text{PO}_4)_3/\text{C}$

材料电化学性能的内在原因,利用 XRD 和 XPS 对比分析了材料循环 100 次后的物质结构及组成。从图 4(A)可以看出, $\text{NaTi}_2(\text{PO}_4)_3/\text{C}$ 材料基于 $1 \text{ mol}\cdot\text{L}^{-1} \text{Na}_2\text{SO}_4$ 电解液循环后的 XRD 样式与原始样式基本相似,但在 17° 左右出现了一个微弱的新峰。这说明材料在低浓度 Na_2SO_4 电解液中循环后的副产物主要以无定形结构存在。当 Na_2SO_4 浓度增加至准饱和状态时,循环后的材料在 15° 和 20° 附近出现了较强的衍射峰。这说明增加电解液浓度有利于晶相副产物生成,与文献结果一致^[27]。当电解液中添加 MgSO_4 后,材料循环后的 XRD 样式与循环前相同,没有出现属于副反应产物的衍射峰,说明 MgSO_4 添加剂显著增强了 $\text{NaTi}_2(\text{PO}_4)_3/\text{C}$ 在硫酸盐电解液中的结构稳定性。图 4(B)展示了 $\text{NaTi}_2(\text{PO}_4)_3/\text{C}$ 材料循环前后的 XPS 谱。结合能位于 465 eV 、 460 eV 的 XPS 峰分别对应于 Ti^{4+} 的 Ti

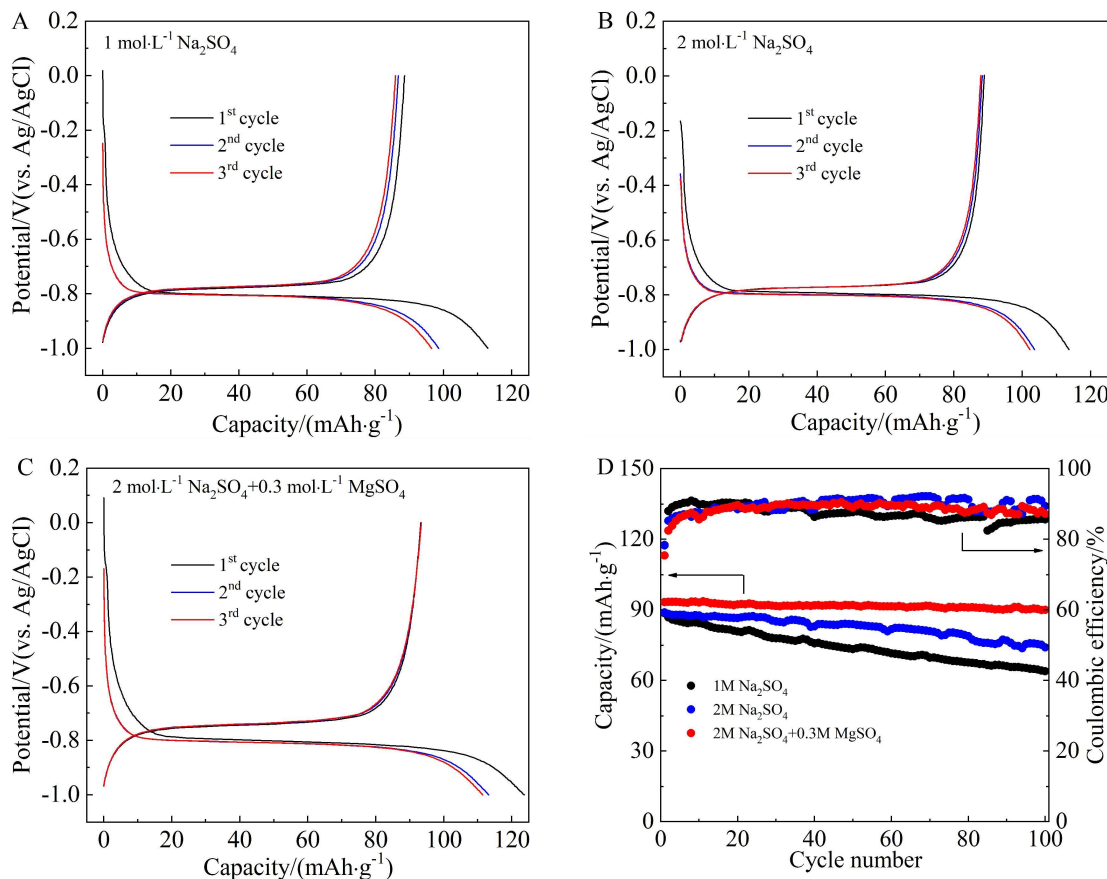


图 3 $\text{NaTi}_2(\text{PO}_4)_3/\text{C}$ 材料基于硫酸盐电解液的充放电曲线:(A) $1 \text{ mol}\cdot\text{L}^{-1} \text{Na}_2\text{SO}_4$; (B) $2 \text{ mol}\cdot\text{L}^{-1} \text{Na}_2\text{SO}_4$; (C) $2 \text{ mol}\cdot\text{L}^{-1} \text{Na}_2\text{SO}_4 + 0.3 \text{ mol}\cdot\text{L}^{-1} \text{MgSO}_4$ 和(D)不同电解液的循环稳定性(网络版彩图)

Figure 3 Charge/discharge profiles of $\text{NaTi}_2(\text{PO}_4)_3/\text{C}$ material in Na_2SO_4 based electrolytes: (A) $1 \text{ mol}\cdot\text{L}^{-1} \text{Na}_2\text{SO}_4$, (B) $2 \text{ mol}\cdot\text{L}^{-1} \text{Na}_2\text{SO}_4$, (C) $2 \text{ mol}\cdot\text{L}^{-1} \text{Na}_2\text{SO}_4 + 0.3 \text{ mol}\cdot\text{L}^{-1} \text{MgSO}_4$, and (D) cycling stability plots in various electrolytes. (color on line)

$2\text{p}_{1/2}$ 和 $\text{Ti } 2\text{p}_{3/2}$ ^[25]。循环后, Ti^{4+} 的结合能几乎没有改变, 且没有出现属于钛基副产物的 XPS 峰, 说明 $\text{NaTi}_2(\text{PO}_4)_3/\text{C}$ 在循环过程中保持了良好的结构稳定性。但是, 循环后, 在 52 eV 附近出现了归因于 Mg^{2+} 的 XPS 峰^[36], 说明循环后材料表面生成了难溶的含 Mg^{2+} 界面保护层。基于以上实验结果, 硫酸盐功能电解液增强材料结构稳定性和电化学性能的作用机制理解如下: 在放电过程中, 电极表面发生电解液析氢副反应, 产生氢氧根离子; 游离在电极表面的 Mg^{2+} 离子即时捕获 OH^- 离子, 在电极表面原位生成难溶的 $\text{Mg}(\text{OH})_2$ 保护层, 从而增强材料的耐腐蚀能力。

为了进一步验证硫酸盐功能电解液的实用性, 采用 $\text{Na}_2\text{Ni}[\text{Fe}(\text{CN})_6]$ 正极、 $\text{NaTi}_2(\text{PO}_4)_3/\text{C}$ 负极和硫酸盐功能电解液($2 \text{ mol}\cdot\text{L}^{-1} \text{Na}_2\text{SO}_4 + 0.3 \text{ mol}\cdot\text{L}^{-1} \text{MgSO}_4$)初步组装了扣式水系钠离子电池, 并测试

了其充放电性能。从图 5 可以看出, 电池在 $100 \text{ mA}\cdot\text{g}^{-1}$ 条件下的可逆容量为 $84.2 \text{ mAh}\cdot\text{g}^{-1}$ (按负极活性物质算)、工作电压约 1.3 V , 比能量接近 $110 \text{ Wh}\cdot\text{kg}^{-1}$ 。在 $500 \text{ mA}\cdot\text{g}^{-1}$ 条件下可逆容量为 $71 \text{ mAh}\cdot\text{g}^{-1}$, 循环 500 次后容量保持率 80%, 展示出了良好的循环稳定性。

4 结 论

水系钠离子电池凭借钠资源丰富、电解液不可燃、能量转换效率高等优点, 在间歇式可再生能源规模储存领域具有应用潜力。NASICON 型 $\text{NaTi}_2(\text{PO}_4)_3/\text{C}$ 是目前最有应用前景的水系钠离子电池负极材料, 但是在传统水系电解液中循环不稳定。通过设计功能添加剂原位构筑耐腐蚀的界面保护层能够有效增强它在水系电解液中的结构稳定性和电化学性能。本论文构建的 $2 \text{ mol}\cdot\text{L}^{-1} \text{Na}_2\text{SO}_4 + 0.3 \text{ mol}\cdot\text{L}^{-1} \text{MgSO}_4$ 新型硫酸盐功能电解

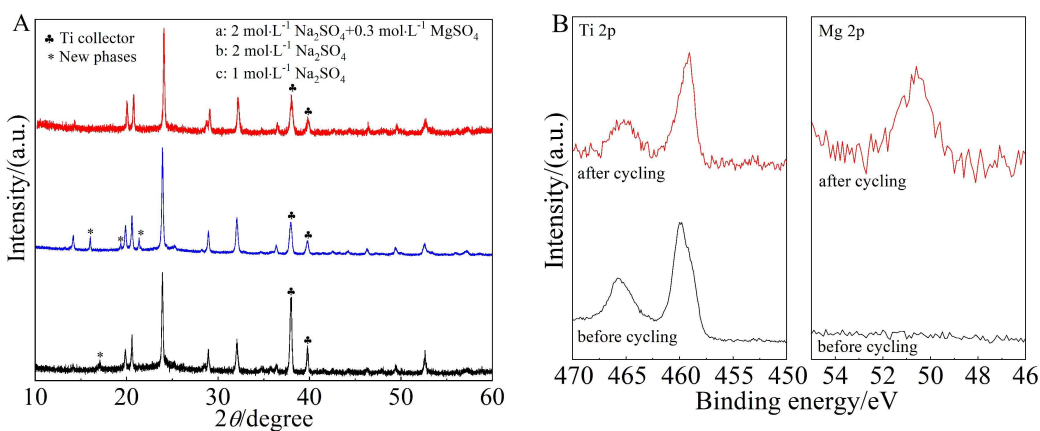


图 4 NaTi₂(PO₄)₃/C 基于硫酸盐电解液充放电循环后的(A)XRD 图和(B)XPS 图 (网络版彩图)

Figure 4 XRD patterns (A) and XPS spectra (B) of NaTi₂(PO₄)₃/C material after being cycled in sulfate-based electrolytes. (color on line)

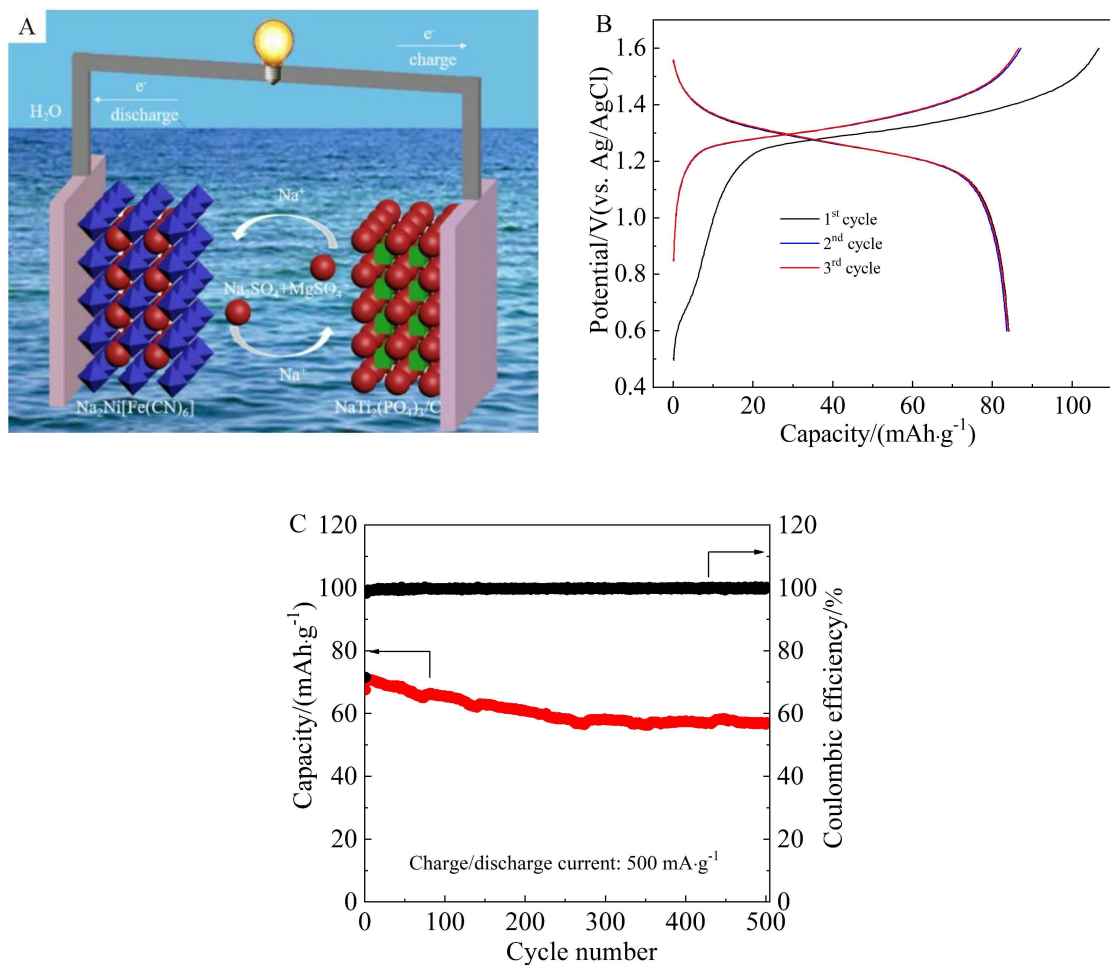


图 5 水系钠离子电池 Na₂Ni[Fe(CN)₆]硫酸盐功能电解液|NaTi₂(PO₄)₃/C 的组装(A)、充放电曲线(B)和循环性能(C)。 (网络版彩图)

Figure 5 Assembling (A), charge/discharge curves (B) and cycle performance (C) of full aqueous sodium-ion batteries with NaTi₂(PO₄)₃/C anode, sulfate electrolyte and Na₂Ni[Fe(CN)₆] cathode. (color on line)

液可以使 $\text{NaTi}_2(\text{PO}_4)_3/\text{C}$ 材料在 $100 \text{ mA} \cdot \text{g}^{-1}$ 条件下稳定循环 100 次以上(容量保持率高达 96.5%)。当前,比能量低和循环寿命不足依然是阻碍水系钠离子电池发展应用的关键。开发能形成稳定电极/电解液界面的水系凝胶电解质是提高水系钠离子电池比能量和循环寿命的重要手段。

参考文献(References):

- [1] Liu SY(刘双), Shao L Y(邵涟漪), Zhang X J(张雪静), Tao Z J(陶占军), Chen J(陈军). Advances in electrode materials for aqueous rechargeable sodium-ion batteries[J]. *Acta Phys. Chim. Sin.*(物理化学学报), 2018, 34(6): 581-597.
- [2] Cao Y(曹翊), Wang Y G(王永刚), Wang Q(王青), Zhang Z Y(张兆勇), Che Y(车勇), Xia Y Y(夏永姚), Dai X(戴翔). Development of aqueous sodium ion battery[J]. *Energy Storage Sci. Tech.*(储能科学与技术), 2016, 5: 317-323.
- [3] Guo Z W, Zhao Y, Ding Y X, Dong X L, Chen L, Cao J Y, Wang C C, Xia Y Y, Peng H S, Wang Y G. Multi-functional flexible aqueous sodium-ion batteries with high safety[J]. *Chem.*, 2017, 3(2): 348-362.
- [4] Liu Y C(刘永畅), Chen C C(陈程成), Zhang N(张宁), Tao Z L(陶占良), Chen J(陈军). Research and application of key materials for sodium ion batteries[J]. *J. Electrochem.*(电化学), 2016, 22(5): 437-452.
- [5] Zhang F, Li W F, Xiang X D, Sun M L. Highly stable Na-storage performance of $\text{Na}_{0.5}\text{Mn}_{0.5}\text{Ti}_{0.5}\text{O}_2$ microrods as cathode for aqueous sodium-ion batteries[J]. *J. Electroanal. Chem.*, 2017, 802: 22-26.
- [6] Wang Y S, Mu L Q, Liu J, Yang Z Z, Yu X Q, Gu L, Hu Y S, Li H, Yang X Q, Chen L Q, Huang X J. A novel high capacity positive electrode material with tunnel-type structure for aqueous sodium-ion batteries[J]. *Adv. Energy Mater.*, 2015, 5(22): 1501005.
- [7] Zhang X Q, Hou Z G, Li X N, Liang J W, Zhu Y C, Qian Y T. Na birnessite with high capacity and long cycle life for rechargeable aqueous sodium-ion battery cathode electrodes[J]. *J. Mater. Chem. A*, 2016, 4(3): 856-860.
- [8] Lin X H(林兴灏), Chi X W(迟晓伟), Liu Y(刘宇), Yang J H(杨建华). $\text{Na}_{3-x}\text{V}_{2-x}\text{Mg}_x(\text{PO}_4)_3$ cathode preparation and its application in aqueous sodium-ion batteries[J]. *Chin. J. Power Sources*(电源技术), 2019, 43: 1821-1824.
- [9] Liu S, Wang L B, Liu J, Zhou M, Nian Q S, Feng Y Z, Tao Z L, Shao L Y. $\text{Na}_3\text{V}_2(\text{PO}_4)_2\text{F}_3$ -SWCNT: a high voltage cathode for non-aqueous and aqueous sodium-ion batteries[J]. *J. Mater. Chem. A*, 2019, 7(1): 248-256.
- [10] Lei P, Wang Y, Zhang F, Wan X, Xiang X D. Carbon-coated $\text{Na}_{2.2}\text{V}_{1.2}\text{Ti}_{0.8}(\text{PO}_4)_3$ cathode with excellent cycling performance for aqueous sodium-ion batteries[J]. *ChemElectroChem*, 2018, 5(17): 2482-2487.
- [11] Fernandez-Ropero A J, Zarabeitia M, Reynaud M, Rojo T, Casas-Cabanas M. Toward safe and sustainable batteries: $\text{Na}_4\text{Fe}_3(\text{PO}_4)_2\text{P}_2\text{O}_7$ as a low cost cathode for rechargeable aqueous Na-ion batteries[J]. *J. Phys. Chem. C*, 2018, 122(1): 133-142.
- [12] Li Y(李勇), He W X(何玮鑫), Zheng X Y(郑芯月), Yu S L(于胜兰), Li H T(李海同), Li H Y(黎弘毅), Zhang R(张蓉), Wang Y(王雨). Prussian blue cathode materials for aqueous sodium-ion batteries: Preparation and electrochemical performance[J]. *J. Inorg. Mater.*(无机材料学报), 2019, 34(4): 365-372.
- [13] Wang W L(王武练), Zhang J(张军), Wang Q S(王秋实), Chen L(陈亮), Wang Z P(王兆平). High-quality $\text{Fe}_4[\text{Fe}(\text{CN})_6]_3$ nanocubes: Synthesis and electrochemical performance as cathode material for aqueous sodium-ion battery[J]. *J. Inorg. Mater.*(无机材料学报), 2019, 34(12): 1301-1308.
- [14] Luo D X, Lei P, Tian G R, Huang Y X, Ren X F, Xiang X D. Insight into electrochemical properties and reaction mechanism of a cobalt-rich Prussian Blue analogue cathode in a NaSO_3CF_3 electrolyte for aqueous sodium-ion batteries[J]. *J. Phys. Chem. C*, 2020, 124(11): 5958-5965.
- [15] Cai D P, Yang X H, Qu B H, Wang T H. Comparison of the electrochemical performance of iron hexacyanoferate with high and low quality as cathode materials for aqueous sodium-ion batteries[J]. *Chem. Commun.*, 2017, 53(50): 6780-6783.
- [16] Zhang Q C, Man P, He B, Li C W, Li Q L, Pan Z H, Wang Z X, Yang J, Wang Z, Zhou Z Y, Lu X H, Niu Z Q, Yao Y G, Wei L. Binder-free $\text{NaTi}_2(\text{PO}_4)_3$ anodes for high-performance coaxial-fiber aqueous rechargeable sodium-ion batteries[J]. *Nano Energy*, 2020, 67: 104212.
- [17] Qiu Y G, Yu Y H, Xu J, Liu Y, Ou M Y, Sun S X, Wei P, Deng Z, Xu Y, Fang C, Li Q, Han J T, Huang Y H. Redox potential regulation toward suppressing hydrogen evolution in aqueous sodium-ion batteries: $\text{Na}_{1.5}\text{Ti}_{1.5}\text{Fe}_{0.5}(\text{PO}_4)_3$ [J]. *J. Mater. Chem. A*, 2019, 7(43): 24953-24963.
- [18] Lei P, Liu K, Wan X, Luo D X, Xiang X D. Ultrafast Na intercalation chemistry of $\text{Na}_2\text{Ti}_{32}\text{Mn}_{12}(\text{PO}_4)_3$ nanodots planted in a carbon matrix as a low cost anode for aqueous sodium-ion batteries[J]. *Chem. Commun.*, 2019, 55(4): 509-512.
- [19] Gu T T, Zhou M, Liu M Y, Wang K L, Cheng S J, Jiang K. A polyimide MWCNTs composite as high capacity anode for aqueous SIBs[J]. *RSC Adv.*, 2016, 6: 53319-53323.

- [20] Deng W W, Shen Y F, Qian J F, Yang H X. A polyimide anode with high capacity and superior cyclability for aqueous Na-ion batteries[J]. *Chem. Commun.*, 2015, 51(24): 5097-5099.
- [21] Wu M G, Ni W, Hu J, Ma J M. NASICON-structured $\text{NaTi}_2(\text{PO}_4)_3$ for sustainable energy storage[J]. *Nano-Micro Lett.*, 2019, 11(1): 44.
- [22] Zheng W T, Lei P, Luo D X, Huang Y X, Tian G R, Xiang X D. Understanding the effect of structural compositions on electrochemical properties of titanium-based polyanionic compounds for superior sodium storage [J]. *Solid State Ionics*, 2020, 345: 115194.
- [23] Malchik F, Shpigel N, Levi M D, Penki T R, Gavriel B, Bergman G, Turgeman M, Aurbach D, Gogotsi Y. MXene conductive binder for improving performance of sodium-ion anodes in water-in-salt electrolyte[J]. *Nano Energy*, 2021, 79: 105433.
- [24] Mohamed A I, Whitacre J F. Capacity fade of $\text{NaTi}_2(\text{PO}_4)_3$ in aqueous electrolyte solutions: Relating pH increases to long term stability[J]. *Electrochim. Acta*, 2017, 235: 730-739.
- [25] Zhan X W, Shirpour M. Evolution of solid/aqueous interface in aqueous sodium-ion batteries[J]. *Chem. Commun.*, 2017, 53(1): 204-207.
- [26] Luo D X, Lei P, Huang Y X, Tian G R, Xiang X D. Improved electrochemical performance of graphene-integrated $\text{NaTi}_2(\text{PO}_4)_3/\text{C}$ anode in high-concentration electrolyte for aqueous sodium-ion batteries[J]. *J. Electroanal. Chem.*, 2019, 838: 66-72.
- [27] Lei P, Li S J, Luo D X, Huang Y X, Tian G R, Xiang X D. Fabricating a carbon-encapsulated $\text{NaTi}_2(\text{PO}_4)_3$ framework as a robust anode material for aqueous sodium-ion batteries[J]. *J. Electroanal. Chem.*, 2019, 847: 113180.
- [28] Li X N, Zhu X B, Liang J W, Hou Z G, Wang Y, Lin N, Zhu Y C, Qian Y T. Graphene-supported $\text{NaTi}_2(\text{PO}_4)_3$ as a high rate anode material for aqueous sodium ion batteries [J]. *J. Electrochem. Soc.*, 2014, 161(6): A1181-A1187.
- [29] Zhang F, Li W F, Xiang X D, Sun M L. Nanocrystal-assembled porous $\text{Na}_3\text{MgTi}(\text{PO}_4)_3$ aggregates as highly stable anode for aqueous sodium-ion batteries[J]. *Chem. Eur. J.*, 2017, 23(52): 12944-12948.
- [30] Gao H C, Goodenough J B. An aqueous symmetric sodium-ion battery with NASICON-structured $\text{Na}_3\text{MnTi}(\text{PO}_4)_3$ [J]. *Angew. Chem. Int. Ed.*, 2016, 55(41): 12768-12772.
- [31] Wang H B, Zhang T R, Chen C, Ling M, Lin Z, Zhang S Q, Pan F, Liang C D. High-performance aqueous symmetric sodium-ion battery using NASICON-structured $\text{Na}_2\text{VTi}(\text{PO}_4)_3$ [J]. *Nano Res.*, 2017, 11(1): 490-498.
- [32] Suo L M, Borodin O, Wang Y S, Rong X H, Sun W, Fan X L, Xu S Y, Schroeder M A, Cresce A V, Wang F, Yang C Y, Hu Y S, Xu K, Wang C S. “Water-in-salt” electrolyte makes aqueous sodium-ion battery safe, green, and long-lasting[J]. *Adv. Energy Mater.*, 2017, 7(21): 1701189.
- [33] Zhang H, Jeong S, Qin B, Carvalho D V, Buchholz D, Passerini S. Towards high-performance aqueous sodium-ion batteries: Stabilizing the solid/liquid interface for NASICON-type $\text{Na}_2\text{VTi}(\text{PO}_4)_3$ using concentrated electrolytes[J]. *ChemSusChem*, 2018, 11(8): 1382-1389.
- [34] Kuhnel R S, Reber D, Battaglia C. A high-voltage aqueous electrolyte for sodium-ion batteries[J]. *ACS Energy Lett.*, 2017, 2(9): 2005-2006.
- [35] Mao W T, Zhang S J, Cao F P, Pan J L, Ding Y M, Ma C, Li M L, Hou Z G, Bao K Y T, Qian Y T. Synthesis of $\text{NaTi}_2(\text{PO}_4)_3@\text{C}$ microspheres by an *in situ* process and their electrochemical properties[J]. *J. Alloys Compd.*, 2020, 842: 155300.
- [36] Zhao Y Y, Wei Z X, Pang Q, Wei Y J, Cai Y M, Fu Q, Du F, Sarapulova A, Ehrenberg H, Liu B B, Chen G. NASICON-type $\text{Mg}_{0.5}\text{Ti}_2(\text{PO}_4)_3$ negative electrode material exhibits different electrochemical energy storage mechanisms in Na-ion and Li-ion batteries[J]. *ACS Appl. Mater. Interfaces*, 2017, 9(5): 4709-4718.

Functional Sulfate Electrolytes Enable the Enhanced Cycling Stability of $\text{NaTi}_2(\text{PO}_4)_3/\text{C}$ Anode Material for Aqueous Sodium-Ion Batteries

Shu-Jin Li, Zhi-Kang Cao, Wen-Kai Wang, Xiao-Han Zhang, Xing-De Xiang*

(College of Chemistry & Chemical Engineering and Resource Utilization,

Northeast Forestry University, Harbin 150040, Heilongjiang, China)

Abstract: Aqueous sodium-ion batteries show promising application in fields of large-scale storage of intermittent renewable energies owing to the earth-abundant sodium resources and incombustible aqueous electrolytes. Primary factors determining whether they can be commercially utilized are low cost and long lifetime. Among current electrode materials, NASICON-type $\text{NaTi}_2(\text{PO}_4)_3$ arouses wide interests as an anode material for aqueous sodium-ion batteries as it offers a high specific capacity, fast Na-transport ability and reasonable working potential, however, suffering from insufficient cycling performance caused by severe dissolution of active materials in traditional aqueous electrolytes. In this work, a functional sulfate electrolyte ($2 \text{ mol}\cdot\text{L}^{-1} \text{Na}_2\text{SO}_4 + 0.3 \text{ mol}\cdot\text{L}^{-1} \text{MgSO}_4$) was designed by coupling concentrated Na_2SO_4 salt and functional MgSO_4 additive to enhance the cycling stability of $\text{NaTi}_2(\text{PO}_4)_3/\text{C}$ material. Experimental results from cyclic voltammetry and galvanostatic measurements suggest that the electrolyte can improve electrochemical reversibility and cycling performance of $\text{NaTi}_2(\text{PO}_4)_3/\text{C}$ material relative to traditional electrolyte ($1 \text{ mol}\cdot\text{L}^{-1} \text{Na}_2\text{SO}_4$). In specific, the material harvested a reversible capacity of $93.4 \text{ mAh}\cdot\text{g}^{-1}$ and impressive capacity retention of 96.5% at the specific current of $100 \text{ mA}\cdot\text{g}^{-1}$ in the functional sulfate electrolyte, but exhibited a reversible capacity of $88.6 \text{ mAh}\cdot\text{g}^{-1}$ and much lower capacity retention of 72.1% in the traditional electrolyte. In order to explore intrinsic causes of the performance improvement, structural properties of the material before and after cycling were comparatively investigated by using X-ray diffraction and X-ray photon spectroscopy. It is found that the material showed excellent structural stability and formation of protective Mg-containing interfacial layer during cycling in the functional sulfate electrolyte. Both the raised electrolyte-salt concentration and functional MgSO_4 additive should be responsible for the enhanced structural stability. The high electrolyte-salt concentration could decrease electrochemical activity and widen electrochemical stability window of electrolyte solvents, while the MgSO_4 additive could timely capture the hydroxyl group resulting from water-solvent decomposition to prevent the alkalization of aqueous electrolytes and spontaneously form protective Mg(OH)_2 interfaces. As a result, the electrolyte could suppress the dissolution of active $\text{NaTi}_2(\text{PO}_4)_3$, thus, resulting in the enhanced structural stability and cycling performance. With an aim to further exhibit the feasibility for practical application, full aqueous sodium-ion batteries were assembled by coupling $\text{Na}_2\text{Ni}[\text{Fe}(\text{CN})_6]$ cathode, functional sulfate electrolyte and $\text{NaTi}_2(\text{PO}_4)_3/\text{C}$ anode. Charge/discharge tests show that the battery could deliver a working voltage of 1.3 V and a reversible capacity of $84.2 \text{ mAh}\cdot\text{g}^{-1}$ (calculated as the mass of active anode material) at the current of $100 \text{ mA}\cdot\text{g}^{-1}$, achieving a specific energy of about $110 \text{ Wh}\cdot\text{kg}^{-1}$. After being continuously charging and discharging for 500 cycles at the current of $500 \text{ mA}\cdot\text{g}^{-1}$, it achieved high capacity retention of 80%. The results in this work suggest that designing functional additive-containing sulfate electrolytes is an effective strategy to fabricate low-cost, long-lifetime aqueous sodium-ion batteries.

Key words: aqueous sodium-ion batteries; anode material; sulfate electrolyte; structural stability; cycling performance